Open Access Full Text Article

ORIGINAL RESEARCH

Antibacterial abilities and biocompatibilities of Ti–Ag alloys with nanotubular coatings

Xingwang Liu,[1] Ang Tian,[2]
Junhua You,[3] Hangzhou Zhang,[4]
Lin Wu,[5] Xizhuang Bai,[1]
Zeming Lei,[1] Xiaoguo Shi,[2]
Xiangxin Xue,[2] Hanning Wang[4]

[1]Department of Orthopedics, The
People's Hospital of China Medical
University, [2]Liaoning Provincial Universities
Key Laboratory of Boron Resource
Ecological Utilization Technology and Boron
Materials, Northeastern University, [3]School
of Materials Science and Engineering,
Shenyang University of Technology, [4]Department of Sports Medicine and Joint
Surgery, The First Affiliated Hospital of
China Medical University, [5]Department of
Prosthodontics, School of Stomatology,
China Medical University, Shenyang,
People's Republic of China

Video abstract

Point your SmartPhone at the code above. If you have a
QR code reader the video abstract will appear. Or use:
http://youtu.be/c_kGIPCT068

Correspondence: Xizhuang Bai
Department of Orthopedics, The People's
Hospital of China Medical University, 33 Wenyi
Road, Shenhe District, Shenyang 110016,
People's Republic of China
Tel +86 24 135 0490 0218
Fax +86 24 2401 6595
Email doctor_baixizhuang@163.com

Purpose: To endow implants with both short- and long-term antibacterial activities without impairing their biocompatibility, novel Ti–Ag alloy substrates with different proportions of Ag (1, 2, and 4 wt% Ag) were generated with nanotubular coverings (TiAg-NT).

Methods: Unlike commercial pure Ti and titania nanotube, the TiAg-NT samples exhibited short-term antibacterial activity against *Staphylococcus aureus* (*S. aureus*), as confirmed by scanning electron microscopy and double staining with SYTO 9 and propidium iodide. A film applicator coating assay and a zone of inhibition assay were performed to investigate the long-term antibacterial activities of the samples. The cellular viability and cytotoxicity were evaluated through a Cell Counting Kit-8 assay. Annexin V-FITC/propidium iodide double staining was used to assess the level of MG63 cell apoptosis on each sample.

Results: All of the TiAg-NT samples, particularly the nanotube-coated Ti–Ag alloy with 2 wt% Ag (Ti2%Ag-NT), could effectively inhibit bacterial adhesion and kill the majority of adhered *S. aureus* on the first day of culture. Additionally, the excellent antibacterial abilities exhibited by the TiAg-NT samples were sustained for at least 30 days. Although Ti2%Ag-NT had less biocompatibility than titania nanotube, its performance was satisfactory, as demonstrated by the higher cellular viability and lower cell apoptosis rate obtained with it compared with those achieved with commercial pure Ti. The Ti1%Ag-NT and Ti4%Ag-NT samples did not yield good cell viability.

Conclusion: This study indicates that the TiAg-NT samples can prevent biofilm formation and maintain their antibacterial ability for at least 1 month. Ti2%Ag-NT exhibited better antibacterial ability and biocompatibility than commercial pure Ti, which could be attributed to the synergistic effect of the presence of Ag (2 wt%) and the morphology of the nanotubes. Ti2%Ag-NT may offer a potential implant material that is capable of preventing implant-related infection.

Keywords: titanium, silver, nanotube, antibacterial, biocompatibility

Introduction

Surgically implanted devices are widely used to improve the patient's quality of life. The most urgent problem faced by orthopedists when using surgically implanted devices is implant-related infection (IRI), which can result in serious complications, such as the need for complex revision procedures, as well as poor prognosis, patient suffering, and even death.[1] Biofilms that are irreversibly attached to device surfaces are the main cause of refractory IRI.[2] The best method for managing IRI is to prevent bacteria from adhering to implant devices and ensure that any adhered bacteria are killed within the initial stage of implant placement.[3] The use of antibiotic-laden bone cement as a local drug delivery system has shown some promise,[4] but the short-lived antibacterial effects caused by the burst release of antibiotics in the initial phase and the bacterial resistance resulting from continuous low-dose antibiotic release in the following phase are difficult limitations to overcome.[5]

Ag-containing inorganic antibiotics, such as silver sulfadiazine and silver nitrate, have well established broad-spectrum antibiotic activities that can be used to manage infections associated with burns and chronic skin wounds.[6] Ag has also been proven effective for the treatment of osteomyelitis and infected nonunions.[7,8] The use of Ag-coated tumor endoprostheses can significantly decrease the rate of deep infection without any adverse effects on liver or renal functions.[9,10] Compared with other inorganic antibiotics, such as Cu and Zn, the antibiotic efficiency of Ag is quite advantageous.[11] Additionally, despite sporadic evidence to the contrary,[12] it is commonly believed that it is difficult for bacterial resistance to develop against Ag ions.[13] Ag can be combined with a variety of implant materials to take advantage of its good mechanical characteristics and processibility.[14]

In recent years, surface modification has been proven an effective method for enhancing the biocompatibility of biomaterials. For example, titania nanotube (TNT) created by the anodization of Ti has been shown to enhance the adhesion and propagation of MC3T3-E1 osteoblasts, and filopodia entering the nanotube pores have been observed to adopt an interlocked cell structure.[15] Furthermore, marrow stromal cells seeded onto TNT show better adhesion, proliferation, early differentiation, and bone matrix deposition compared with those seeded onto commercial pure titanium (cp-Ti).[16] TNT also exhibits enhanced biocompatibility in vivo; for example, it has been reported that peri-implant bone formation and bone development are improved by the implantation of TNT into the frontal skulls of pigs.[17]

The suppression of biofilm formation, prolongation of antibacterial activity without the development of bacterial resistance, and maintenance of favorable biocompatibility are expected to be achieved through the fabrication of nanotubes on the Ti–Ag alloy surface. Moreover, compared with TNT loaded with Ag nanoparticles, this study sintered Ag and Ti together in their entirety instead of using the postloading technique, thereby eliminating the risk that Ag could disengage from the nanotubes. Thus, the TiAg-NT samples should exhibit more sustainable and reliable antibacterial ability, and the concern regarding the hazards caused by free nanoparticles should be decreased. In the current study, we investigated the antibacterial ability and biocompatibility of nanotube-coated Ti–Ag alloys with varying proportions of Ag.

Materials and methods
Nanotube fabrication
A previously described protocol was used to coat Ti–Ag substrates with nanotubes.[18] In brief, cp-Ti and Ti–Ag sintered alloy slices (1, 2, and 4 wt% Ag) that measured 14 mm in diameter and 2 mm in thickness were polished, washed in acetone, and ultrasonically cleaned for 30 minutes. The plates were washed three times with deionized water and then dried in a stream of nitrogen gas. A two-step anodization process was then applied to fabricate the nanotubes. During this process, the plates were first anodized under a constant voltage of 60 V for 2 hours in an ethanediol solution containing 0.5 wt% ammonium fluoride, cleaned in hydrochloric acid, dried in nitrogen gas, and then anodized under a constant voltage of 20 V for 4 hours. Platinum slices were used as a counter electrode. The nanotube coatings were then thermally treated at 450°C in air to obtain a stable crystal phase.

Surface characterization
Field-emission scanning electron microscopy (SEM, SU8010, Hitachi Ltd., Tokyo, Japan) was employed to observe the surface morphologies of the samples. The chemical composition and concentrations in each sample were determined through energy dispersive spectroscopy (SwiftED3000, Hitachi Ltd.). The crystalline structures of the samples were determined by X-ray diffraction (D/max2400, Rigaku, Tokyo, Japan). The surface roughness was tested by confocal laser scanning microscopy (LEXT OLS4100, Olympus Corporation, Tokyo, Japan), and the water contact angle of each sample at room temperature was measured using image collection and analysis systems (DataPhysics OCA20; DataPhysics Instruments GmbH, Stuttgart, Germany) with distilled water as the determining medium.[19]

Ag ion release
To measure the release of Ag ions, the TiAg-NT samples were immersed in 10 mL of a 0.9% NaCl solution at 37°C for 120 hours. The Ag ions released into the solution were analyzed through inductively coupled plasma mass spectrometry (ICP-MS, Optima 5300DV, PerkinElmer Inc., Waltham, MA, USA) with an accuracy of 0.01 mg/L.

Electrochemical analysis
An electrochemical analysis was performed to determine the anticorrosion properties of each sample. To perform this analysis, the cp-Ti, TNT, and TiAg-NT samples were sealed with their nanotube surfaces exposed. Electrochemical tests were conducted at 37°C in a beaker containing 100 mL of simulated body fluid. An electrochemical workstation (CHI660E, Shanghai Chenhua Co., Ltd, Shanghai, People's Republic of China) was used to investigate the corrosion behavior. A standard three-electrode system with saturated calomel as a reference and a platinum electrode as a counter were used.[20]

Antibacterial assays

The antibacterial activity against *Staphylococcus aureus* (*S. aureus* N315, supplied by the Microbiology Department of China Medical University) was tested. *S. aureus* bacteria were cultivated in a brain heart infusion medium at 37°C for 18 hours and then diluted to a concentration of 10^5 CFU/mL for the antibacterial assays.

Short-term antibacterial ability

The short-term antibacterial ability was determined by SEM (S4800, Hitachi Ltd.) and double staining with SYTO 9 and propidium iodide (PI). To perform this analysis, the samples were arranged in a 24-well plate and immersed in 1 mL of a bacterial suspension at a concentration of 10^5 CFU/mL. After culturing for 1 day, any nonadherent bacteria on the surface were removed by washing with phosphate-buffered saline (PBS), and the samples were subsequently fixed with a 2.5% glutaraldehyde solution (Solarbio, Beijing, People's Republic of China) for 2 hours at 4°C. After two washes with PBS, the samples were dehydrated in an ethanol series (50%, 60%, 70%, 80%, 90%, 95%, and 100%; 15 minutes per solution) and then dried at room temperature. After the samples were critical-point dried, the adherent bacteria on the samples were coated with Au and subjected to SEM.[21]

Following the seeding procedure described earlier, after culturing for 1 day, the specimens were rinsed twice with PBS, double-stained with SYTO 9 and PI (LIVE/DEAD BacLight Bacterial Viability Kits, Thermo Fisher Scientific, Waltham, MA, USA) for 15 minutes in darkness, and examined using a confocal laser scanning microscopy (FV1000, Olympus Corporation).[22]

Long-term antibacterial ability

After the samples were sterilized and immersed in 10 mL of PBS at 37°C for 30 days with fresh PBS being replaced every day, the long-term antibacterial activity against *S. aureus* was tested using a film applicator coating assay and a zone of inhibition assay (ZOI).[23] The film applicator coating assay was used to evaluate the long-term antibacterial activity based on the National Standard of China (QB/T 2591-2003). To perform this assay, 90 μL of the bacterial suspension was dripped onto the surface of each sample. After incubation at 37°C and 90% humidity for 1 day, each sample was washed carefully with 1 mL of PBS and ultrasonically agitated to detach all bacteria from the surface. After standard serial dilution and plate counting, the antibacterial rate was calculated according to the following formula: $AR = (A - B)/A \times 100\%$, where AR is the antibacterial rate, A is the mean number of viable bacteria on the cp-Ti sample, and B is the mean number of viable bacteria on the TNT and TiAg-NT samples.

The ZOI assay was also utilized for the evaluation of antibacterial ability according to the National Standard of China (QB/T 2738–2005). To perform this assay, an agar solution was distributed evenly onto 100-mm Petri dishes and cooled to room temperature under sterile conditions. The *S. aureus* suspension was then sprayed over each Petri dish, and aseptic cp-Ti, TNT, and TiAg-NT samples were separately placed into two dishes. The Petri dishes were then incubated for 24 hours at 37°C and 90% humidity, and the antibacterial properties of the samples were assessed by evaluating the width of the inhibition zone formed around each sample.[24]

Biocompatibility assays

The MG63 cell line (The Cell Bank of Type Culture Collection of Chinese Academy of Sciences, Shanghai, People's Republic of China), which is derived from a human bone osteosarcoma, was used for the biocompatibility assays. For these assays, the cells were cultured in high-glucose Dulbecco's Modified Eagle Medium (DMEM; Thermo Fischer Scientific, Waltham, MA, USA) with 10% fetal bovine serum (PAN-Biotech GmbH, Aidenbach, Germany) and 1% penicillin-streptomycin (Thermo Fisher Scientific) under standard conditions (95% humidity, 5% CO_2, and 37°C). The culture medium was replaced every other day, and the cells were passaged once they reached 80% confluence.

Cell viability and cytotoxicity

The cell viability was examined using a Cell Counting Kit-8 assay (CCK-8; Dojindo, Kumamoto, Japan) according to previously described procedures with minor modifications.[25] Briefly, 1 mL of a cell suspension at a density of 7×10^5 cells/mL was seeded onto each sample. After culturing for 1, 3, and 5 days, all of the samples were transferred into new 24-well plates and washed twice with PBS. Then, 1 mL of fresh DMEM and 0.1 mL of Cell Counting Kit-8 assay solution were added into each well, and the plates were incubated for 3 hours. Formazan-class dyes were detected by measuring the absorbance at 450 nm using a microplate reader (Power-Wave XS, BIOTEC, Winooski, VT, USA). At the same time, the relative growth rate (RGR) was calculated according to the following formula: $RGR = OD_{sample}/OD_{cp-Ti} \times 100\%$. According to the National Chinese Standard (Gb/T 16886.5-2003), an RGR value $\geq 100\%$ is considered level 0, an RGR value between 75% and 99% is considered level 1, an RGR value between 50% and 74% is considered level 2, an RGR value between 25% and 49% is considered level 3, an

RGR value between 1% and 24% is considered level 4, and an RGR value ≤0% is considered level 5. Levels 0 and 1 are noncytotoxic, level 2 mildly cytotoxic, level 3 moderately cytotoxic, and levels 4 and 5 markedly cytotoxic.

Annexin V-FITC/PI staining

Aliquots of 1 mL of the cell suspensions were seeded onto each sample at a concentration of 7×10^5 cells/mL. After culturing in an incubator for 1, 4, and 7 days, the cells on each sample were harvested, washed twice with ice-cold PBS, resuspended in $1 \times$ binding buffer, and stained with Annexin V-FITC for 15 minutes in darkness and with PI for 5 minutes on ice (7Sea Pharmatech Co., Ltd., Shanghai, People's Republic of China). The cells were then analyzed by flow cytometry. The Annexin V+/PI− (early apoptotic) or Annexin V+/PI+ (late apoptotic) cells were considered apoptotic. The flow cytometry data were analyzed using WinMDI 2.9 software.

Statistical analysis

The assays were processed in triplicate, and each experiment was repeated three times. The experimental results are expressed as the mean ± standard deviations. A one-way analysis of variation combined with the Student–Newman–Keuls post hoc test was adopted to determine the level of significance. $P < 0.05$ was regarded as significant and $P < 0.01$ highly significant.

Results

Surface characterization

Figure 1 displays SEM images of the TNT, Ti1%Ag-NT, Ti2%Ag-NT, and Ti4%Ag-NT samples. The nanotubes formed by anodization at 20 V exhibited a diameter of ~20 nm. The Ag contents of the Ti1%Ag-NT, Ti2%Ag-NT, and Ti4%Ag-NT samples according to energy dispersive spectroscopy were 0.95±0.025 wt%, 1.93±0.025 wt%, and 3.91±0.02 wt%, respectively. Figure 2 shows the X-ray diffraction patterns formed by the different materials. Peaks specifically corresponding to Ti could be observed in the cp-Ti sample, and higher-intensity diffraction peaks of TiO_2 were also observed in the TNT sample. In addition, peaks corresponding to Ag_2O and TiAg could be observed next to the peaks of the TiO_2 phase in the
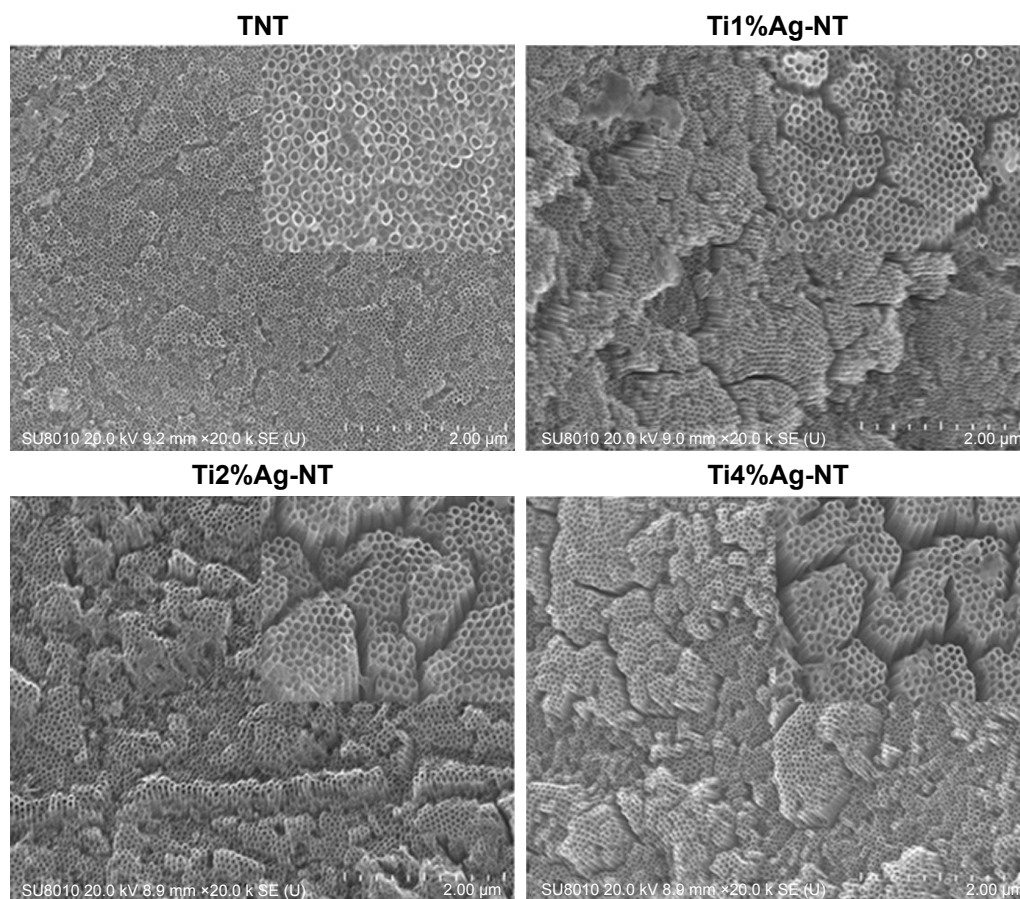
Figure 1 SEM views of the nanotubes (NT) formed on the surfaces of the TNT, Ti1%Ag-NT, Ti2%Ag-NT, and Ti4%Ag-NT samples with insets showing higher-magnification (60.0 k SE[U]).
Abbreviations: SEM, scanning electron microscopy; TNT, titania nanotube.
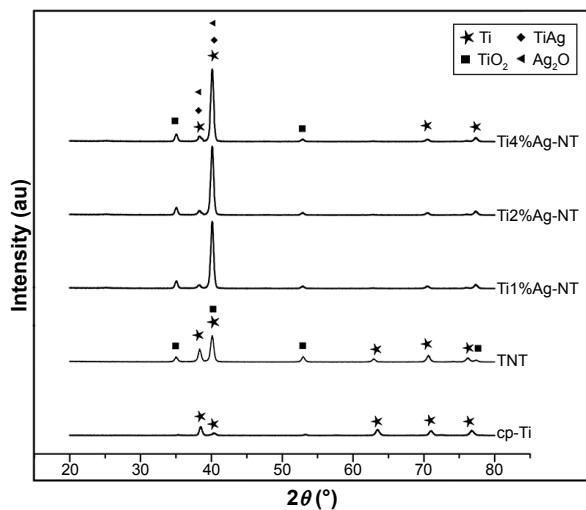
Figure 2 XRD patterns of the cp-Ti, TNT, and TiAg-NT samples.
Abbreviations: XRD, X-ray diffraction; cp-Ti, commercial pure titanium; TNT, titania nanotubes; TiAg-NT, TiAg alloys with nanotubular coverings.

TiAg-NT samples. Collectively, the SEM, X-ray diffraction, and energy dispersive spectroscopy results indicated that nanotubes successfully formed on the Ti–Ag alloy substrates with an average diameter of 20 nm and that the Ag atoms on the surfaces of these substrates were oxidized into Ag ions. As shown in Table 1 and Figures 3 and 4, the surface roughness of TNT and TiAg-NT samples was markedly higher than that of cp-Ti ($P<0.01$). Increasing the Ag concentration improved the surface roughness of the TiAg-NT samples, although this trend was not significant ($P>0.05$). A wettability test was performed to reveal the differences among these samples, as shown in Figure 5, and cp-Ti and TNT had the largest and smallest contact angles, respectively. The analysis of the TiAg-NT samples revealed that the contact angle increased with an increase in the Ag concentration, and the contact angle of Ti4%Ag-NT was two-fold greater than that of Ti1%Ag-NT and 1.7-fold greater than that of Ti2%Ag-NT ($P<0.01$). Thus, the hydrophilicity followed the order TNT>Ti1%Ag-NT> Ti2%Ag-NT>Ti4%Ag-NT>cp-Ti.

Table 1 Surface roughness of the cp-Ti, TNT, and TiAg-NT samples determined by CLSM (mean ± SD)

Groups	Ra (μm)	Rq (μm)	Rz (μm)
cp-Ti	0.1±0.0109	0.133±0.0208	0.831±0.2242
TNT	0.209±0.0138	0.26±0.0143	1.486±0.086
Ti1%Ag-NT	0.225±0.0055	0.276±0.0204	1.412±0.1574
Ti2%Ag-NT	0.264±0.0446	0.325±0.0612	1.52±0.3061
Ti4%Ag-NT	0.285±0.0349	0.351±0.0421	1.72±0.2476

Abbreviations: CLSM, confocal laser scanning microscopy; cp-Ti, commercial pure titanium; Ra, arithmetical mean deviation; Rq, root mean square deviation; Rz, ten-point height; TNT, titania nanotubes; TiAg-NT, TiAg alloys with nanotubular coverings.

Anticorrosion properties and Ag-ion release

Figure 6 shows the typical Tafel curves obtained for the cp-Ti, TNT, and TiAg-NT samples. The Ecorr for the cp-Ti sample was greater than those for the TNT and TiAg-NT samples. Furthermore, the corrosion current density obtained for the cp-Ti sample was lower than those obtained for the TNT and TiAg-NT samples. These results confirmed that corrosion occurred on the TNT and TiAg-NT samples. Additionally, the TNT and TiAg-NT samples showed more corrosion than the cp-Ti sample. Moreover, the release of Ag ions was evaluated by ICP-MS and less than 0.01 mg/L Ag ions were detected.

Short-term antibacterial ability

Figure 7 shows SEM images of *S. aureus* cells seeded onto the samples after culturing for 1 day. The cp-Ti and TNT samples were similar in appearance: both were fully covered with a multilayered *S. aureus* biofilm. In contrast, only scattered bacteria were detected on the surfaces of the TiAg-NT samples, and the Ti2%Ag-NT sample was nearly free of bacteria.

SYTO 9 is a specific dye for living bacteria, which are stained green in its presence. Conversely, PI is a specific dye that stains dead bacteria red. As shown in Figure 8, far fewer viable bacteria were found on the TiAg-NT samples than the cp-Ti and TNT samples after 1 day of culture. Only a few living bacteria were observed on the Ti1%Ag-NT and Ti4%Ag-NT samples, and almost no living bacteria were observed on the Ti2%Ag-NT sample. Moreover, the low fluorescence signal produced by the Ti2%Ag-NT sample confirmed that this sample had the fewest bacteria adhering to it.

Long-term antibacterial ability

After immersion in PBS for 30 days, the cp-Ti, TNT, and TiAg-NT samples were seeded with *S. aureus* and incubated for 1 day. As shown in Figure 9, many *S. aureus* colonies were observed on the cp-Ti and TNT samples. In contrast, far fewer colonies were found on the Ti1%Ag-NT and Ti4%Ag-NT samples, and virtually no bacterial colonies were detected on the Ti2%Ag-NT sample. The antibacterial ratios of the Ti1%Ag-NT, Ti2%Ag-NT, and Ti4%Ag-NT samples were 95%±2.5%, 98%±1%, and 91%±2.1%, respectively. Moreover, as shown in Figure 10, no inhibition zones could be found surrounding any of the samples.

Cell viability and cytotoxicity

MG63 cells were seeded onto each sample, incubated for 1, 3, and 5 days and subjected to a Cell Counting Kit-8 assay.
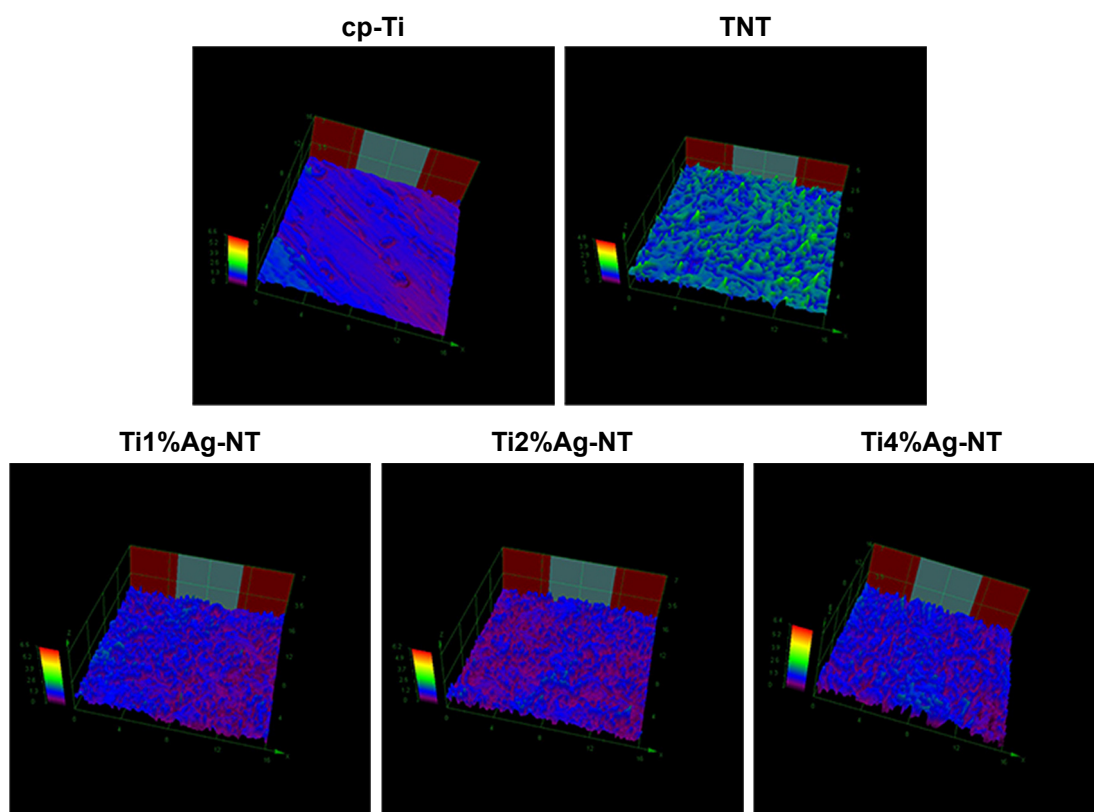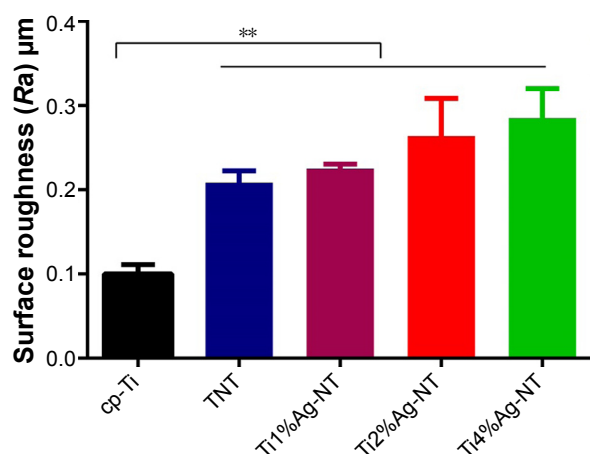
Figure 3 CLSM images of the surfaces of the cp-Ti, TNT, and TiAg-NT samples.
Abbreviations: CLSM, confocal laser scanning microscopy; cp-Ti, commercial pure titanium; TNT, titania nanotubes; TiAg-NT, TiAg alloys with nanotubular coverings.

As shown in Figure 11, a constant increase in the optical density (OD) value was observed from day 1 to 5 for all of the samples with the exception of the Ti4%Ag-NT sample, which showed a decrease in the OD value from day 3 to 5. The TNT sample presented the greatest cell viability at all of the tested time points ($P<0.01$). The Ti2%Ag-NT sample showed equally good viability as the cp-Ti sample on days 1 and 5 ($P>0.05$) but significantly higher cell viability than the cp-Ti sample on day 3 ($P<0.01$). The Ti1%Ag-NT and Ti4%Ag-NT samples showed worse cell viability than the cp-Ti sample ($P<0.01$). Collectively, the above-presented results showed that the TNT sample resulted in the highest

Figure 4 Surface roughness (Ra) of the cp-Ti, TNT, and TiAg-NT samples.
Notes: **$P<0.01$. Results expressed as mean ± SD (ANOVA on all groups).
Abbreviations: cp-Ti, commercial pure titanium; TNT, titania nanotubes; TiAg-NT, TiAg alloys with nanotubular coverings; ANOVA, analysis of variance.
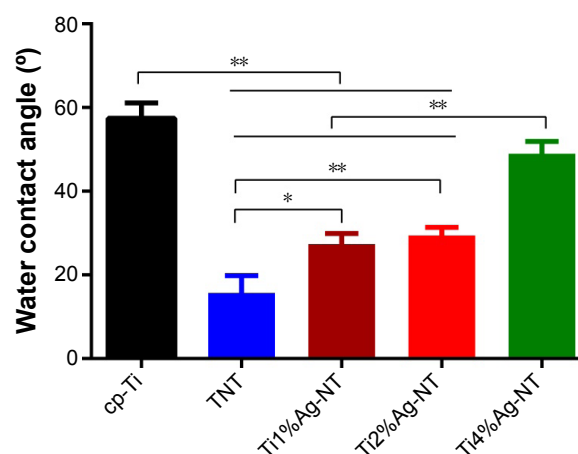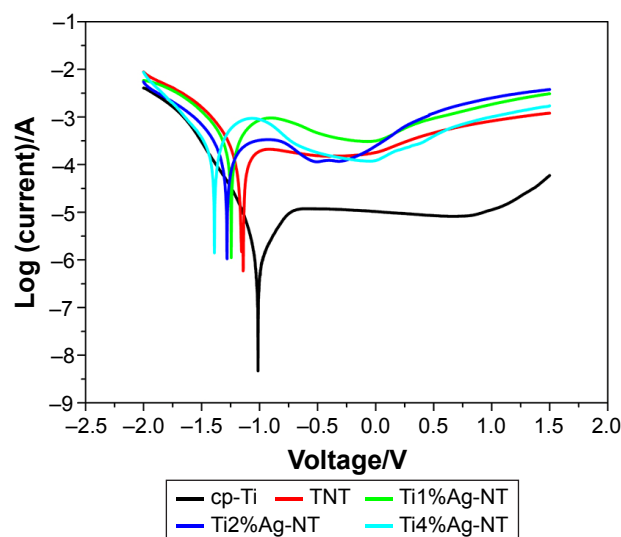

Figure 5 Water contact angles of the cp-Ti, TNT, and TiAg-NT samples.
Notes: *$P<0.05$, **$P<0.01$. Results expressed as mean ± SD (ANOVA on all groups).
Abbreviations: cp-Ti, commercial pure titanium; TNT, titania nanotubes; TiAg-NT, TiAg alloys with nanotubular coverings; ANOVA, analysis of variance.

Figure 6 Tafel curves of the cp-Ti, TNT, and TiAg-NT samples.
Abbreviations: cp-Ti, commercial pure titanium; TNT, titania nanotubes; TiAg-NT, TiAg alloys with nanotubular coverings.

cell viability, followed by the Ti2%Ag-NT sample and then the cp-Ti, Ti1%Ag-NT, and Ti4%Ag-NT samples. The RGRs calculated for all of the samples are listed in Table 2. The RGRs of the cp-Ti, TNT, Ti1%Ag-NT, and Ti2%Ag-NT samples from day 1 to 5 were all level 0 or 1, but the RGR of the Ti4%Ag-NT sample reached level 2 at day 5. These results indicated that the cp-Ti, TNT, Ti1%Ag-NT, and Ti2%Ag-NT samples were noncytotoxic at all of the tested

time points, whereas the Ti4%Ag-NT sample was mildly cytotoxic at day 5.

Annexin V-FITC/PI staining

Apoptosis is a natural event that occurs at all cell types. The apoptotic behavior of MG63 cells after culturing on each sample for 1, 4, and 7 days was determined through a flow cytometric analysis. As shown in Figures 12 and 13, a one-fold increase in the apoptotic rate was observed from day 1 to 7 when the cells were cultured on the cp-Ti, TNT, and Ti4%Ag-NT samples. The Ti2%Ag-NT and Ti1%Ag-NT samples yielded two- and three-fold increases in the apoptotic rates, respectively. The cp-Ti sample exhibited the highest apoptosis rates on both day 1 and 7 ($P<0.01$). Higher numbers of apoptotic cells were observed on the TNT and Ti2%Ag-NT samples on day 4; however, the differences between the cp-Ti sample and the anodized samples, including the TNT and TiAg-NT samples, were not significant ($P>0.05$). Overall, the apoptosis rates of MG63 cells on the TNT, Ti1%Ag-NT, Ti2%Ag-NT, and Ti4%Ag-NT samples were lower than that of the cells on the cp-Ti sample.

Discussion

Ag coatings have been applied to various medical prostheses, such as vascular, urinary, and orthopedic devices, and to peritoneal catheters and sutures for the prevention
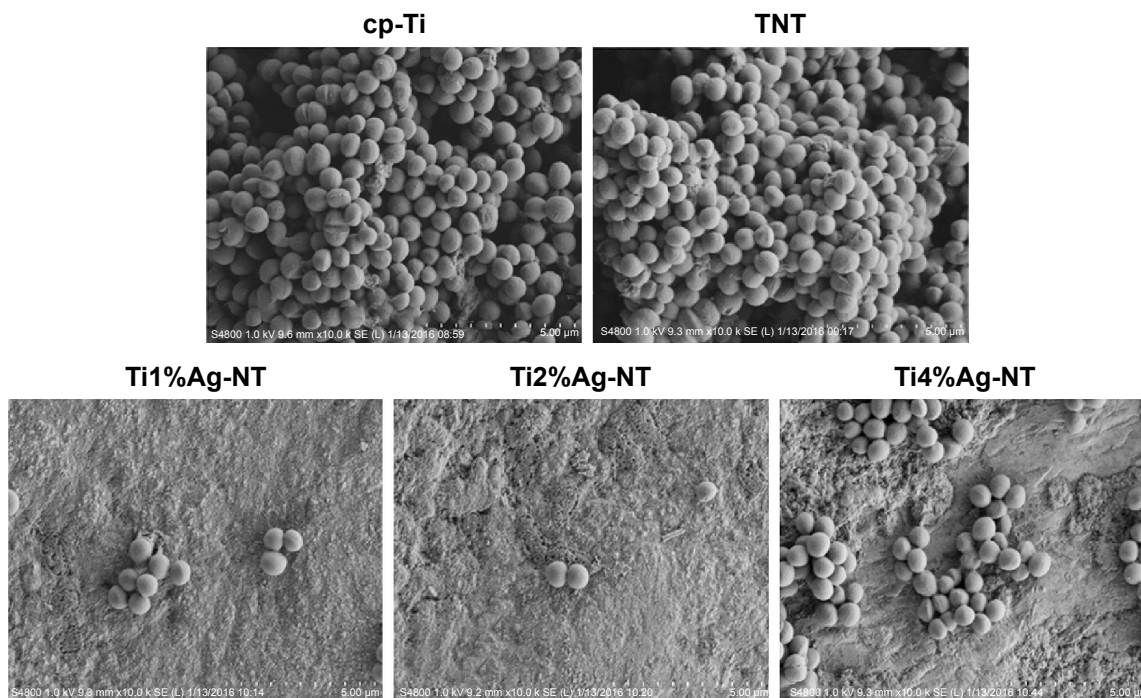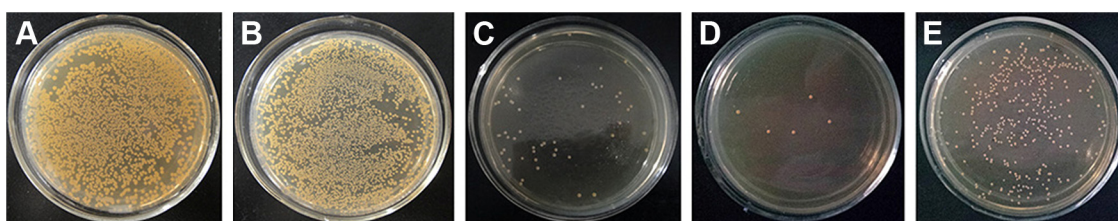

Figure 7 SEM images of *Staphylococcus aureus* cells after incubation for 1 day on the cp-Ti, TNT, and TiAg-NT samples.
Abbreviations: cp-Ti, commercial pure titanium; TNT, titania nanotubes; TiAg-NT, TiAg alloys with nanotubular coverings; SEM, scanning electron microscopy.
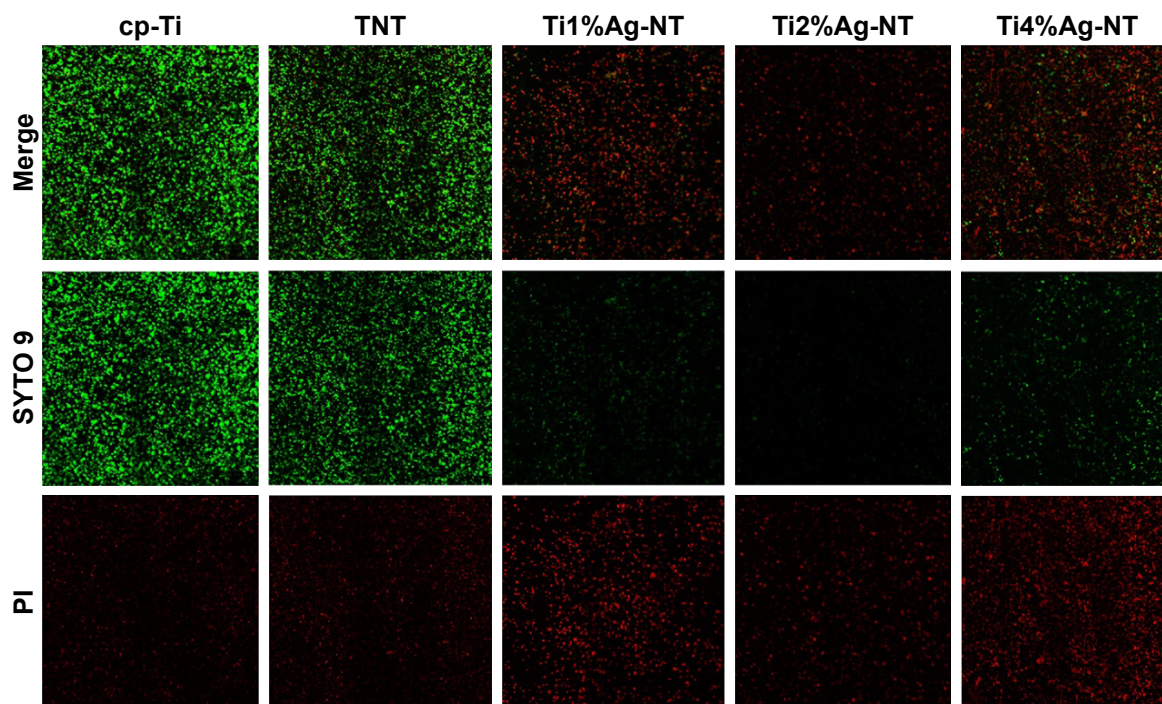
Figure 8 CLSM images of *Staphylococcus aureus* cells stained with SYTO 9 and PI after 1 day of culture on the cp-Ti, TNT, and TiAg-NT samples.
Abbreviations: CLSM, confocal laser scanning microscopy; cp-Ti, commercial pure titanium; PI, propidium iodide; TNT, titania nanotubes; TiAg-NT, TiAg alloys with nanotubular coverings.

Figure 9 *Staphylococcus aureus* colonies collected from the cp-Ti (**A**), TNT (**B**), Ti1%Ag-NT (**C**), Ti2%Ag-NT (**D**), and Ti4%Ag-NT (**E**) samples.
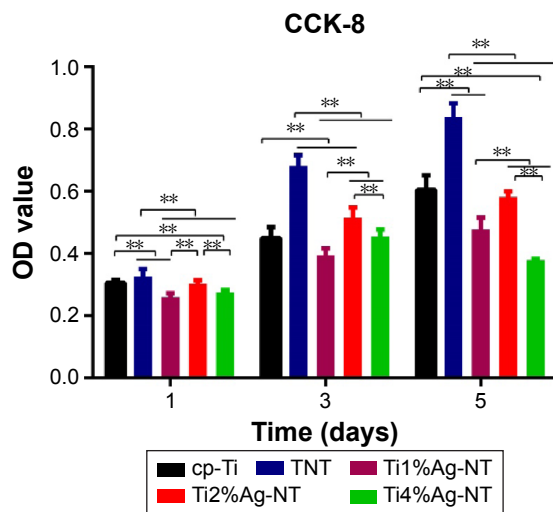**Abbreviations:** cp-Ti, commercial pure titanium; TNT, titania nanotubes; TiAg-NT, TiAg alloys with nanotubular coverings.
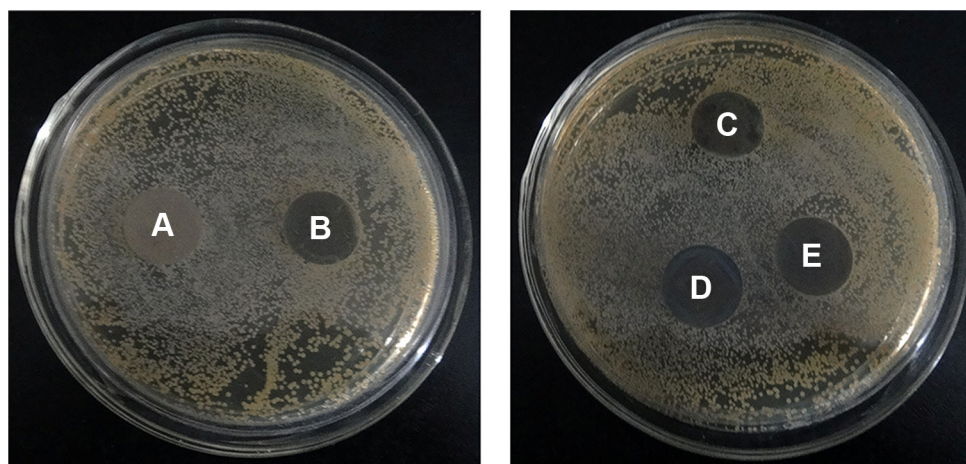
Figure 10 No inhibition zones could be found surrounding the cp-Ti (**A**), TNT (**B**), Ti1%Ag-NT (**C**), Ti2%Ag-NT (**D**), or Ti4%Ag-NT (**E**) samples.
Abbreviations: cp-Ti, commercial pure titanium; TNT, titania nanotubes; TiAg-NT, TiAg alloys with nanotubular coverings.

Figure 11 Optical Density (OD) values of MG63 cells after 1, 3, and 5 days of culture on the cp-Ti, TNT, and TiAg-NT samples.
Notes: **$P<0.01$. Results expressed as mean ± SD (ANOVA on all groups).
Abbreviations: CCK-8, Cell Counting Kit-8 assay; cp-Ti, commercial pure titanium; TNT, titania nanotubes; TiAg-NT, TiAg alloys with nanotubular coverings; ANOVA, analysis of variance.

of IRI.[26,27] Furthermore, these coatings impart favorable biocompatibility to biomaterials, which is indispensable for their successful application.[10,28] In the current study, we coated a Ti–Ag alloy with nanotubular coatings to obtain a new biomaterial that exhibits an advantageous antibacterial ability and biocompatibility.

The Ag ions released by coated substrates are hypothesized to impart antibacterial properties.[22,29] As shown in Figure 2, the observed formation of Ag_2O proved that Ag ions were present in our samples. Indeed, the corrosion of the TiAg-NT samples, which was verified by electrochemical testing, inevitably led to the release of Ag ions into the surrounding environment. However, the released Ag ions were not detectable by ICP-MS, which might be due to the low Ag content (1%, 2%, and 4 wt% Ag, respectively) and the limited sensitivity of ICP-MS (limit of detection of 0.01 mg/L). The antibacterial nature of Ag ions has

Table 2 RGRs and cytotoxic levels of the cp-Ti, TNT, and TiAg-NT samples with regard to MG63 cells after 1, 3, and 5 days in culture

Groups	1 day		3 days		5 days	
	RGR (%)	Level	RGR (%)	Level	RGR (%)	Level
cp-Ti	100	0	100	0	100	0
TNT	106.89	0	151.74	0	138.96	0
Ti1%Ag-NT	85.14	1	87.68	1	79.19	1
Ti2%Ag-NT	99.45	1	114.77	0	96.41	1
Ti4%Ag-NT	90.05	1	101.19	0	62.69	2

Abbreviations: cp-Ti, commercial pure titanium; RGR, relative growth rate; TNT, titania nanotubes; TiAg-NT, TiAg alloys with nanotubular coverings.

been known since the time of Avicenna,[30] but the mechanisms underlying this property remain largely unknown. Dosunmu et al suggested that the antibacterial ability of Ag-coated carbon nanotubes is attributable to the effect of Ag ions on cell-membrane integrity, their downregulation of the expression of virulence-associated genes, and their induction of general and oxidative stress.[31] Furthermore, Gordon et al showed that the antibacterial property of Ag ions is based on their inactivation of key enzymes, such as succinate dehydrogenase, mediated by their binding to thiol groups and on their induction of hydroxyl radical formation, which results in DNA damage.[32]

Because it is the most common pathogen resulting in IRI,[20] *S. aureus* was used in the current study to evaluate the antimicrobial properties of our samples. Biofilm formation is the primary cause of IRI because it enables bacteria to escape from antibiotics and the host immune system.[33,34] Initial bacterial adhesion is the first step in biofilm formation and the only step that can be inhibited; as such, it is critical that the substrates used in the clinic retain their antibacterial properties from their first day of use. As shown in Figure 7, few bacteria grew on the TiAg-NT samples after 1 day of culture, indicating that these samples could effectively inhibit bacterial colonization. This result is consistent with those obtained in a study reported by Kramer et al who demonstrated that the inhibition of bacterial colonization is a significant feature of Ag ions.[35] Furthermore, to verify the bactericidal effects of the TiAg-NT samples, the samples were seeded with bacteria and subjected to double staining with SYTO 9 and PI. As shown in Figure 8, large numbers of living bacteria were detected on the cp-Ti and TNT samples, whereas the vast majority of the bacteria seeded on the TiAg-NT samples were dead. In addition, the low fluorescence intensity observed on the Ti2%Ag-NT sample proved that this sample harbored few bacteria on its surface, consistent with the SEM results discussed above. Collectively, these results demonstrated that the TiAg-NT samples, particularly the Ti2%Ag-NT sample, exhibited strong antibacterial properties. Indeed, this sample not only inhibited bacterial adhesion but also induced the death of adhered bacteria.

Due to hematogenous infection or chronic low-virulence infection,[36] IRI may occur months or even years after surgery; therefore, it is crucial to endow implants with long-term antibacterial activity. Before performing long-term antibacterial tests on our samples, the samples were soaked in PBS for 1 month with daily replacement of the PBS.[23] Our film applicator coating assay test results, which are shown in Figure 9, revealed that the antibacterial abilities
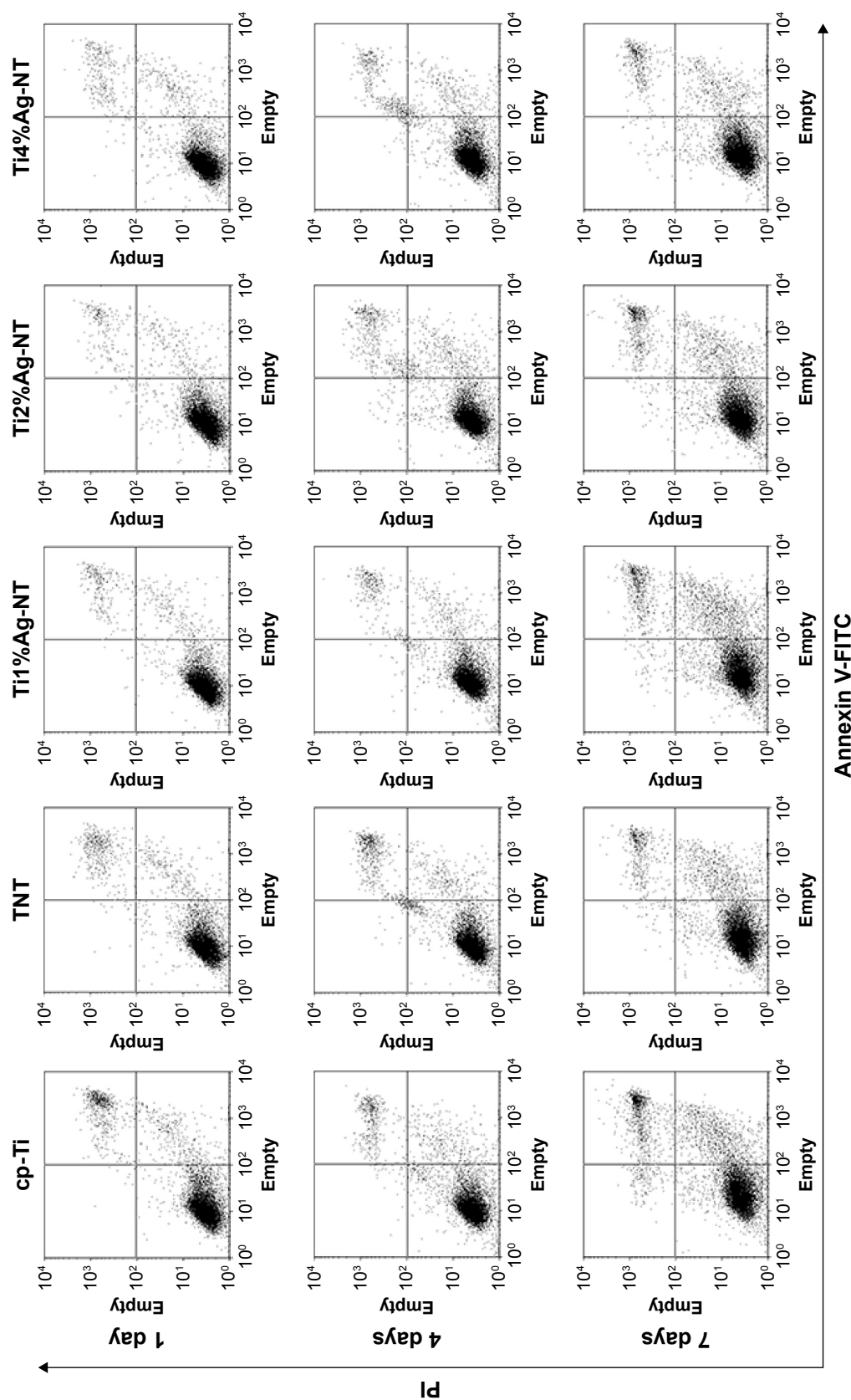
Figure 12 Flow cytometric analysis of MG63 cell apoptosis after 1, 4, and 7 days of culture on the cp-Ti, TNT, and TiAg-NT samples.
Abbreviations: cp-Ti, commercial pure titanium; PI, propidium iodide; TNT, titania nanotubes; TiAg-NT, TiAg alloys with nanotubular coverings.
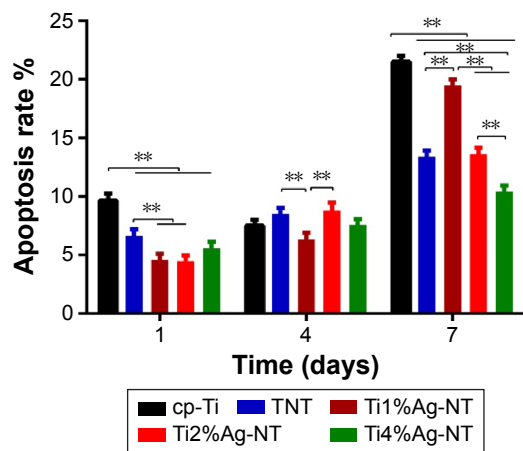
Figure 13 Apoptosis rates of MG63 cells after culture on the cp-Ti, TNT, and TiAg-NT samples for 1, 4, and 7 days.
Notes: **$P<0.01$. Results expressed as mean $\pm$ SD (ANOVA on all groups).
Abbreviations: cp-Ti, commercial pure titanium; TNT, titania nanotubes; TiAg-NT, TiAg alloys with nanotubular coverings; ANOVA, analysis of variance.

of the TiAg-NT samples ($>90\%$) were sustained for at least 1 month. This prolonged effect was attributed to the combination of the limited release of Ag ions, which was verified by ICP-MS, and the high antibacterial efficacy of Ag ions. Mahltig et al demonstrated that Ag ions can exhibit antibacterial activity even when released in limited quantities.[11] After implantation, Ag ions would be released from an implant substrate due to corrosion caused by bodily fluids, wear, and mechanically accelerated electrochemical processes.[37] As such, the TiAg-NT samples should exert a markedly longer antibacterial effect than might be expected; indeed, this effect might theoretically continue until the end of an implant's life.

In addition to Ag ions, the antibacterial property of each sample is also regulated by the surface roughness and hydrophilicity. Increased hydrophilicity results in increased antibacterial performance due to higher surface energy, as has been demonstrated by an increasing number of studies.[19,38,39] As shown in Table 1 and Figures 3 and 4, compared with TNT, the surface roughness of the TiAg-NT samples increased slowly with an increase in the Ag content, and the differences among the samples were insignificant ($P>0.05$). As shown in Figure 5, the TiAg-NT samples were less hydrophilic than TNT, and decreased hydrophilicity was obtained with an increase in the Ag content. This finding is consistent with the results of the study conducted by Mei et al who showed that Ag undermines the surface hydrophilicity.[22] With similar surface roughness and hydrophilicity ($P>0.05$), Ti2%Ag-NT exhibited better antibacterial properties than Ti1%Ag-NT, and this should be attributed to its higher Ag content. However, Ti4%Ag-NT, which had a higher Ag content than

Ti2%Ag-NT, showed a lower antibacterial property, likely because the hydrophilicity of Ti4%Ag-NT was significantly worse than that of Ti2%Ag-NT ($P<0.01$), and the influence on antibacterial performance resulting from the difference in hydrophilicity was higher than that resulting from the difference in the Ag content between the two samples. Overall, the final antibacterial performance of each sample is the sum of the effect of Ag ions and the effect of hydrophilicity. Thus, Ti2%Ag-NT exhibited improved antibacterial property than both Ti1%Ag-NT and Ti4%Ag-NT.

In ZOI assays, inhibition zones form due to the burst release of antibiotics. The absence of inhibition zones obtained in the ZOI assays in the current study proved that Ag ions were not being burst-released from the TiAg-NT samples but rather released slowly and in limited quantities. Collectively, the aforementioned results showed that the TiAg-NT samples were only effective for adhered bacteria. This finding is similar to the results obtained in research conducted by Zheng et al who presented similar ZOI and ICP-MS results and showed that only bacteria in direct contact with an implant substrate could be killed.[39] It should also be noted that because the accumulation of Ag ions in blood, liver, and kidneys is detrimental,[40] the limited release of Ag ions from the samples observed in this study could suggest that Ag will not accumulate in organs, minimizing its potential cytotoxicity.[41,42]

The biomaterials used for implants should not only possess excellent antibacterial effects but also offer beneficial biocompatibility. In the current study, the MG63 cell line, which is derived from a human bone osteosarcoma with a typical osteoblast phenotype, was used to evaluate the biocompatibilities of the various samples.

Cp-Ti is biocompatible and widely used in the clinic, which led us to use it as a benchmark to evaluate the biocompatibilities of the TiAg-NT samples. As shown in Figures 11–13, the Ti2%Ag-NT sample exhibited better cell viability and lower apoptosis rate than the cp-Ti sample. This difference has two potential explanations: 1) the 2 wt% Ag sample had low cytotoxicity. According to research reported by Chen et al, co-sputtered Ag-HA coatings with 2.05±0.55 wt% Ag show good biocompatibility and cause no cytotoxicity to osteoblast precursor cells.[43] 2) The morphology of the nanotubes enhanced the biocompatibility of the sample surfaces, concordant with previous results.[16,44,45] For example, in our previous study, nanotubes measuring 20 nm in diameter were optimal for promoting cellular adhesion, migration, and proliferation.[18] The nanoroughness of a surface could also impart favorable biocompatibility. According to a theory proposed by Zhao et al, sample surfaces coated

with nanotubes could possess nanotopographies that promote osteoconductivity, which is advantageous from a biomimetic viewpoint.[46] Another positive feature of nanotubes is their hydrophilicity, which is very important for the initial adhesion of osteoblasts to a substrate.[47] Finally, the connecting space that exists between nanotube walls allows the exchange of nutrients, gas, and cell signaling molecules even after cells reach confluency.[48]

Excess Ag ions are known to exert adverse effects on human cells.[49,50] With the higher Ag content and relatively worse hydrophilicity, Ti2%Ag-NT unexpectedly exhibited better biocompatibility than Ti1%Ag-NT, and this finding might be explained by the result demonstrated by Zhang et al who showed that the influence of mental ions on biocompatibility is not dose-dependent and that the Ti-10Cu (wt%) is more biocompatible than Ti-5Cu (wt%).[51] Moreover, Ti4%Ag-NT was found to be less biocompatible than Ti2%Ag-NT, a finding that could be explained by its significantly worse hydrophilicity ($P<0.01$). The limited improvement in biocompatibility produced by the low hydrophilicity of Ti4%Ag-NT could not compensate for the cytotoxicity produced by its Ag ions; therefore, as shown in Table 2, Ti4%Ag-NT was mildly cytotoxic at day 5.

Conclusion

In the current study, the TiAg-NT samples with varying proportions of Ag (1, 2, and 4 wt% Ag) were fabricated. These materials showed strong antibacterial ability that was sustained for at least 30 days. The Ti2%Ag-NT sample exhibited the highest efficiency in inhibiting biofilm formation and also presented the most favorable biocompatibility, as shown by their maintenance of high cell viability and low apoptosis rate compared with cp-Ti. Thus, Ti2%Ag-NT is a promising new antibacterial biomaterial.

Limitations

According to the electrochemical test results, the TiAg-NT samples showed poorer anticorrosion properties than the cp-Ti sample, suggesting that the TiAg-NT samples might shorten an implant's life. The biocompatibilities of the TiAg-NT samples need to be further studied both in vitro and in vivo.

Acknowledgments

Disclosure

The authors report no conflicts of interest in this work.

References

1. Zhao L, Chu PK, Zhang Y, Wu Z. Antibacterial coatings on titanium implants. *J Biomed Mater Res B Appl Biomater*. 2009;91(1): 470–480.
2. Donlan RM, Costerton JW. Biofilms: survival mechanisms of clinically relevant microorganisms. *Clin Microbiol Rev*. 2002;15(2):167–193.
3. Tamilvanan S, Venkateshan N, Ludwig A. The potential of lipid- and polymer-based drug delivery carriers for eradicating biofilm consortia on device-related nosocomial infections. *J Control Release*. 2008; 128(1):2–22.
4. Kelm J, Regitz T, Schmitt E, Jung W, Anagnostakos K. In vivo and in vitro studies of antibiotic release from and bacterial growth inhibition by antibiotic-impregnated polymethylmethacrylate hip spacers. *Antimicrob Agents Chemother*. 2006;50(1):332–335.
5. Neut D, van de Belt H, van Horn JR, van der Mei HC, Busscher HJ. Residual gentamicin-release from antibiotic-loaded polymethylmethacrylate beads after 5 years of implantation. *Biomaterials*. 2003;24(10):1829–1831.
6. Klasen HJ. A historical review of the use of silver in the treatment of burns. II. renewed interest for silver. *Burns*. 2000;26(2):131–138.
7. Mostafavi HR, Tornetta P 3rd. Open fractures of the humerus treated with external fixation. *Clin Orthop Relat Res*. 1997;337:187–197.
8. Becker RO, Spadaro JA. Treatment of orthopaedic infections with electrically generated silver ions. A preliminary report. *J Bone Joint Surg Am*. 1978;60(7):871–881.
9. Hardes J, von Eiff C, Streitbuerger A, et al. Reduction of periprosthetic infection with silver-coated megaprostheses in patients with bone sarcoma. *J Surg Oncol*. 2010;101(5):389–395.
10. Hardes J, Ahrens H, Gebert C, et al. Lack of toxicological side-effects in silver-coated megaprostheses in humans. *Biomaterials*. 2007;28(18): 2869–2875.
11. Mahltig B, Soltmann U, Haase H. Modification of algae with zinc, copper and silver ions for usage as natural composite for antibacterial applications. *Mater Sci Eng C Mater Biol Appl*. 2013;33(2): 979–983.
12. Landsdown AB, Williams A. Bacterial resistance to silver in wound care and medical devices. *J Wound Care*. 2007;16(1):15–19.
13. Percival SL, Bowler PG, Russell D. Bacterial resistance to silver in wound care. *J Hosp Infect*. 2005;60(1):1–7.
14. Nakajo K, Takahashi M, Kikuchi M, et al. Inhibitory effect of Ti-Ag alloy on artificial biofilm formation. *Dent Mater J*. 2014;33(3):389–393.
15. Oh S, Daraio C, Chen LH, Pisanic TR, Finones RR, Jin S. Significantly accelerated osteoblast cell growth on aligned TiO_2 nanotubes. *J Biomed Mater Res A*. 2006;78(1):97–103.
16. Popat KC, Leoni L, Grimes CA, Desai TA. Influence of engineered titania nanotubular surfaces on bone cells. *Biomaterials*. 2007;28(21): 3188–3197.
17. von Wilmowsky C, Bauer S, Lutz R, et al. In vivo evaluation of anodic TiO2 nanotubes: an experimental study in the pig. *J Biomed Mater Res B Appl Biomater*. 2009;89(1):165–171.

18. Tian A, Qin X, Wu A, et al. Nanoscale TiO$_2$ nanotubes govern the biological behavior of human glioma and osteosarcoma cells. *Int J Nanomedicine*. 2015;10:2423–2439.

19. Shi X, Tian A, Tian Y, et al. Antibacterial activities of TiO2 nanotubes on Porphyromonas gingivalis. *RSC Adv*. 2015;5:34237–34242.

20. Liu J, Li F, Liu C, et al. Effect of Cu content on the antibacterial activity of titanium-copper sintered alloys. *Mater Sci Eng C Mater Biol Appl*. 2014;35:392–400.

21. Cheng H, Li Y, Huo K, Gao B, Xiong W. Long-lasting in vivo and in vitro antibacterial ability of nanostructured titania coating incorporated with silver nanoparticles. *J Biomed Mater Res A*. 2014;102(10):3488–3499.

22. Mei S, Wang H, Wang W, et al. Antibacterial effects and biocompatibility of titanium surfaces with graded silver incorporation in titania nanotubes. *Biomaterials*. 2014;35(14):4255–4265.

23. Gao A, Hang R, Huang X, et al. The effects of titania nanotubes with embedded silver oxide nanoparticles on bacteria and osteoblasts. *Biomaterials*. 2014;35(13):4223–4235.

24. Zhang E, Li F, Wang H, et al. A new antibacterial titanium-copper sintered alloy: preparation and antibacterial property. *Mater Sci Eng C Mater Biol Appl*. 2013;33(7):4280–4287.

25. Li L, Pan S, Zhou X, et al. Reduction of in-stent restenosis risk on nickel-free stainless steel by regulating cell apoptosis and cell cycle. *PLoS One*. 2013;8(4):e62193.

26. Darouiche RO. Anti-infective efficacy of silver-coated medical prostheses. *Clin Infect Dis*. 1999;29(6):1371–1377; quiz 1378.

27. Bosetti M, Masse A, Tobin E, Cannas M. Silver coated materials for external fixation devices: in vitro biocompatibility and genotoxicity. *Biomaterials*. 2002;23(3):887–892.

28. Campoccia D, Montanaro L, Arciola CR. A review of the biomaterials technologies for infection-resistant surfaces. *Biomaterials*. 2013;34(34):8533–8554.

29. Kumar R, Munstedt H. Silver ion release from antimicrobial polyamide/silver composites. *Biomaterials*. 2005;26(14):2081–2088.

30. Secinti KD, Ayten M, Kahilogullari G, Kaygusuz G, Ugur HC, Attar A. Antibacterial effects of electrically activated vertebral implants. *J Clin Neurosci*. 2008;15(4):434–439.

31. Dosunmu E, Chaudhari AA, Singh SR, Dennis VA, Pillai SR. Silver-coated carbon nanotubes downregulate the expression of Pseudomonas aeruginosa virulence genes: a potential mechanism for their antimicrobial effect. *Int J Nanomedicine*. 2015;10:5025–5034.

32. Gordon O, Vig Slenters T, Brunetto PS, et al. Silver coordination polymers for prevention of implant infection: thiol interaction, impact on respiratory chain enzymes, and hydroxyl radical induction. *Antimicrob Agents Chemother*. 2010;54(10):4208–4218.

33. Costerton JW, Stewart PS, Greenberg EP. Bacterial biofilms: a common cause of persistent infections. *Science*. 1999;284(5418):1318–1322.

34. Albers CE, Hofstetter W, Siebenrock KA, Landmann R, Klenke FM. In vitro cytotoxicity of silver nanoparticles on osteoblasts and osteoclasts at antibacterial concentrations. *Nanotoxicology*. 2013;7(1):30–36.

35. Kramer SJ, Spadaro JA, Webster DA. Antibacterial and osteoinductive properties of demineralized bone matrix treated with silver. *Clin Orthop Relat Res*. 1981;161:154–162.

36. Portillo ME, Salvado M, Alier A, et al. Prosthesis failure within 2 years of implantation is highly predictive of infection. *Clin Orthop Relat Res*. 2013;471(11):3672–3678.

37. Matusiewicz H. Potential release of in vivo trace metals from metallic medical implants in the human body: from ions to nanoparticles – a systematic analytical review. *Acta Biomater*. 2014;10(6):2379–2403.

38. Puckett SD, Taylor E, Raimondo T, Webster TJ. The relationship between the nanostructure of titanium surfaces and bacterial attachment. *Biomaterials*. 2010;31(4):706–713.

39. Zheng Y, Li J, Liu X, Sun J. Antimicrobial and osteogenic effect of Ag-implanted titanium with a nanostructured surface. *Int J Nanomedicine*. 2012;7:875–884.

40. Wan AT, Conyers RA, Coombs CJ, Masterton JP. Determination of silver in blood, urine, and tissues of volunteers and burn patients. *Clin Chem*. 1991;37(10 Pt 1):1683–1687.

41. Brutel de la Riviere A, Dossche KM, Birnbaum DE, Hacker R. First clinical experience with a mechanical valve with silver coating. *J Heart Valve Dis*. 2000;9(1):123–129; discussion 129–130.

42. Langanki D, Ogle MF, Cameron JD, Lirtzman RA, Schroeder RF, Mirsch MW. Evaluation of a novel bioprosthetic heart valve incorporating anticalcification and antimicrobial technology in a sheep model. *J Heart Valve Dis*. 1998;7(6):633–638.

43. Chen W, Liu Y, Courtney HS, et al. In vitro anti-bacterial and biological properties of magnetron co-sputtered silver-containing hydroxyapatite coating. *Biomaterials*. 2006;27(32):5512–5517.

44. Rani VV, Vinoth-Kumar L, Anitha VC, Manzoor K, Deepthy M, Shantikumar VN. Osteointegration of titanium implant is sensitive to specific nanostructure morphology. *Acta Biomater*. 2012;8(5):1976–1989.

45. Ma QL, Zhao LZ, Liu RR, et al. Improved implant osseointegration of a nanostructured titanium surface via mediation of macrophage polarization. *Biomaterials*. 2014;35(37):9853–9867.

46. Zhao L, Wang H, Huo K, et al. Antibacterial nano-structured titania coating incorporated with silver nanoparticles. *Biomaterials*. 2011;32(24):5706–5716.

47. Liu XH, Wu L, Ai HJ, Han Y, Hu Y. Cytocompatibility and early osseointegration of nanoTiO$_2$-modified Ti-24 Nb-4 Zr-7.9 Sn surfaces. *Mater Sci Eng C Mater Biol Appl*. 2015;48:256–262.

48. Brammer KS, Frandsen CJ, Jin S. TiO$_2$ nanotubes for bone regeneration. *Trends Biotechnol*. 2012;30(6):315–322.

49. Cho Lee AR, Leem H, Lee J, Park KC. Reversal of silver sulfadiazine-impaired wound healing by epidermal growth factor. *Biomaterials*. 2005;26(22):4670–4676.

50. Fraser JF, Cuttle L, Kempf M, Kimble RM. Cytotoxicity of topical antimicrobial agents used in burn wounds in Australasia. *ANZ J Surg*. 2004;74(3):139–142.

51. Zhang E, Zheng L, Liu J, Bai B, Liu C. Influence of Cu content on the cell biocompatibility of Ti-Cu sintered alloys. *Mater Sci Eng C Mater Biol Appl*. 2015;46:148–157.